Fall 12-3-2010

Design, synthesis and SAR of a new class of small molecule inhibitors of β-Secretase.

Jordan M. Anderson
University of South Florida

Design, synthesis and SAR of a new class of small molecule inhibitors of β-Secretase.

Jordan M. Anderson

Honors Thesis

Approved : December 03, 2010

Design, synthesis, and SAR of a new class of small molecule inhibitors of β-Secretase.

Jordan M. Anderson
Honors Thesis, University of South Florida.

Abstract

β-Secretase is the enzyme responsible for the Amyloid-β plaques found in Alzheimer's disease. Inhibition of this enzyme should prove to be very useful in combating Alzheimer's disease by preventing this build-up. After a computational screening of the NCID-2 library a molecule was found to possess a 2- propanol structure with aromatic groups on either side. This moiety was replicated by a combinatorial library of 150 compounds. These compounds were screened initially against β-secretase at 100, 50, and then 25 μM to narrow down to 17 structures showing 50% inhibition at 25 μM. The IC50 for each of the 17 molecules was found experimentally resulting in one lead compound **15**, 4.93 μM ± 0.86 μM. This compound was modified by making slight changes to the 2-propanol moiety resulting in mostly loss of activity.

Introduction

Alzheimer's disease (AD) currently affects 4-8 % of the population above 65. Or about 3-5 million people in the US, making it the most common cause of dementia in elderly people. This number is projected to raise from to 25 million patients by 2050 (1). Symptoms of Alzheimer's disease include memory loss, paranoia, delusions, and declining in language function (5). Although there has been some controversy to what is the cause of AD, there is a strong consensus on the lesions that are characteristic of an AD inflicted brain. First are the intracellular neurofibrillary tangles, helical filaments formed from a hypophosphorylated form of tau. Lastly there are extracellular plaques from deposits of amyloid-β peptide.

These deposits are formed by the cleavage of an amyloid precursor protein (APP) by β-secretase. There are two mechanisms of APP cleavage that may occur. First in the wild type environment amyloid-β is created first by the cleavage of the amyloid precursor protein by β-secretase to form the N-terminus and then γ-secretase finish off the cleavage releasing the mature Aβ peptide. The second pathway is used in the environment without β-secretase present. In this case α-secretase can preform the same function as β-secretase (1). Although the Aβ peptide is created by three proteins, only β-secretase cleaves specifically at the Asp +1

and Glu +11. γ-Secretase cleaves the APP into a range of peptides from 38 to 43 residues, but the $A\beta_{40}$ is the major product at 90% abundance. Albeit a minor product $A\beta_{42}$, at 9% abundance, has been shown to be the more pathogenic peptide, giving the most to plaque formation (5, 3).

β-Secretase was discovered in 1992 and was immediately proposed as a target for Alzheimer's disease. It wasn't definitively characterized until 1999 when it was identified by five different research groups using different methods. It was named differently by the different groups names included BACE (Vasser et al, 1999), β-Secretase, (Sinha et al., 1999), Asp2 (Hussain et al., 1999; Yan et al., 1999), and memapsin 2 (Lin et al., 2000) (1, 3).

Although many researchers focus drug discovery towards finding the inhibitor with the lowest IC50, or binding affinity. This is only part of whether a compound can become a useable drug. The main cause of concern with a prospective drug molecule is other properties of the drug with in the patient including bioavailability and pharmicotoxic effects.

β-Secretase showed to remain a good drug target not only because of the evidence between amyloid-β plaques and Alzheimer's, but also because mice lacking the gene to produce β-secretase showed no amyloid-β and initially demonstrated no adverse side effects. Although more recents studies with β-secretase knockout mice showed a decrease in the myelin sheath layers in both peripheral and central nervous cells (2). When further investigated it was found that in the early stages of development, when these sheaths first form, the concentration of β-secretase was increased when compared to that at latter stages in life. This is proposed to occur by the cleavage of Neuregulin1 by β-secretase, whose product is a growth and differentiation factor that leads to the formation of the myelin sheath. β-Secretase knockout mice were found to have the full length neuregulin1 peptide almost exclusively, while wild type mice had a mixture between it an the smaller products. This causes decreased hippocampal synaptic plasticity, decreased cognitive performance, and reduce lifespan (2). By nature β-secretase knockout mice imitates inhibition for the entire life cycle. Inhibition of β-secretase only latter in life, when Alzheimer's disease predominantly occurs, cannot be measured this way. These side effects could only occur because of the high rate of myelination happening during development.

Fluorescence Resonance Energy Transfer (FRET)

One of the most difficult problems to overcome when designing a drug is being able to find the relevant biological activity of compounds

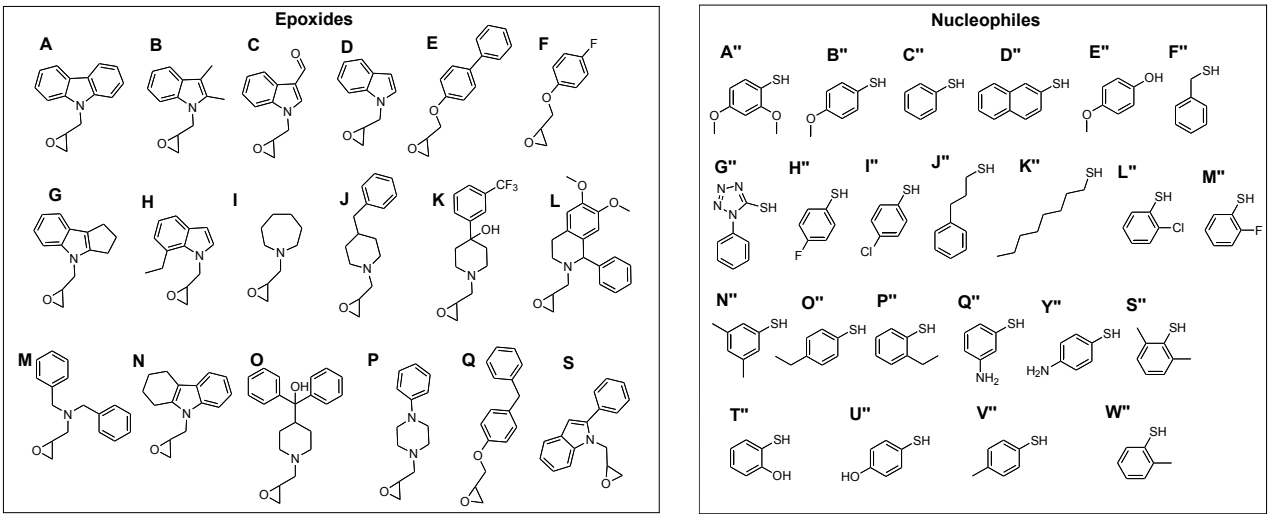

Figure 1:
Shows the building blocks used to create the combinatorial library. Each molecule is referenced by the epoxide opening reaction between the two building blocks used.

synthesized. Since β-Secretase is an enzyme there is already a biologically relevant reaction taking place. A Fluorescence Resonance Energy Transfer (FRET) assay takes advantage of this reaction to allow for the detection of compounds that would inhibit this enzyme's active site. The natural substrate of the enzyme (a peptide chain) is modified by first adding a fluorescent donor to one side of the molecule and a fluorescent acceptor to the other side of the chain. When this complete molecule is excited by light the fluorescent acceptor effectively quenches the donor by resonance energy transfer and no emission is seen by the detector. β-Secretase naturally cleaves this peptide substrate. When this substrate is cleaved the donor and acceptor are no longer in resonance energy transfer with each other and thus when the donor fluorophore is excited by the light it is no longer quenched by the acceptor and thus fluoresces (Figure 1). This emission can be detected by a fluorometer, and the intensity of the light emitted is directly proportional to the amount of substrate being cleaved. If an inhibitor is placed in with the substrate and the protein, the effectiveness of the inhibitor and the intensity of the light would be inversely related. By varying the concentration of the inhibitor FRET becomes a powerful tool in determining the IC_{50} values of the compounds. This value represents the concentration needed for the 50% inhibition of the binding site.

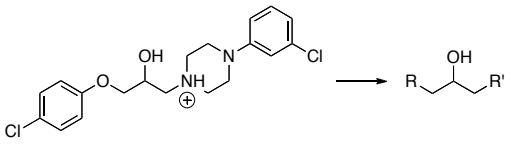

Figure 2:
Demonstrates the relationship between the NCID-2 hit to the combinatorial library synthesized.

Results

The initial lead compound was found after computational screening of the NCID-2 library, of

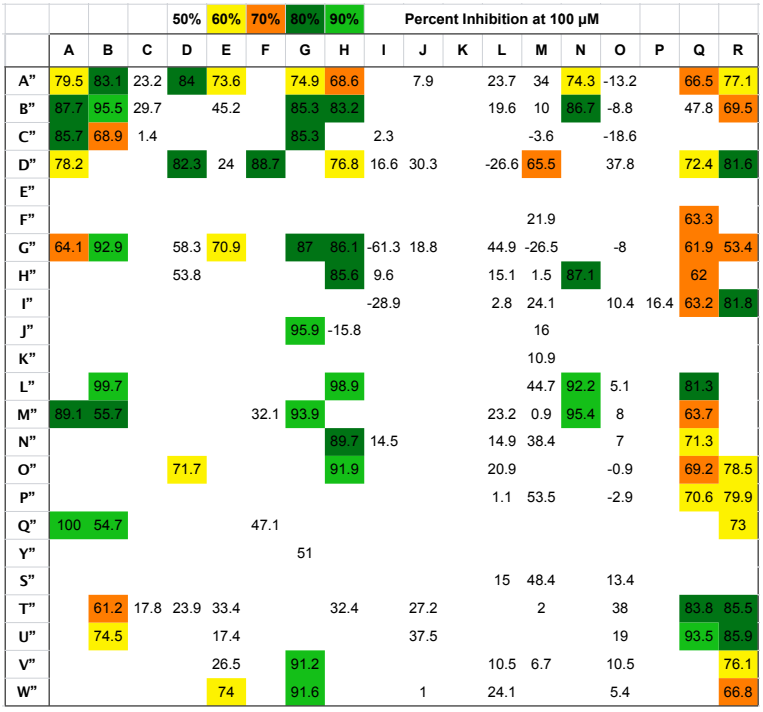

	A	B	C	D	E	F	G	H	I	J	K	L	M	N	O	P	Q	R
A”	79.5	83.1	23.2	84	73.6		74.9	68.6		7.9		23.7	34	74.3	-13.2		66.5	77.1
B”	87.7	95.5	29.7		45.2		85.3	83.2				19.6	10	86.7	-8.8		47.8	69.5
C”	85.7	68.9	1.4				85.3		2.3				-3.6		-18.6			
D”	78.2			82.3	24	88.7		76.8	16.6	30.3		-26.6	65.5		37.8		72.4	81.6
E”																		
F”													21.9				63.3	
G”	64.1	92.9		58.3	70.9		87	86.1	-61.3	18.8		44.9	-26.5		-8		61.9	53.4
H”				53.8				85.6	9.6			15.1	1.5	87.1			62	
I”									-28.9			2.8	24.1		10.4	16.4	63.2	81.8
J”							95.9	-15.8					16					
K”													10.9					
L”		99.7						98.9					44.7	92.2	5.1		81.3	
M”	89.1	55.7				32.1	93.9					23.2	0.9	95.4	8		63.7	
N”								89.7	14.5			14.9	38.4		7		71.3	
O”				71.7				91.9				20.9			-0.9		69.2	78.5
P”												1.1	53.5		-2.9		70.6	79.9
Q”	100	54.7				47.1												73
Y”							51											
S”												15	48.4		13.4			
T”		61.2	17.8	23.9	33.4			32.4		27.2			2		38		83.8	85.5
U”		74.5			17.4					37.5					19		93.5	85.9
V”					26.5		91.2					10.5	6.7		10.5			76.1
W”					74		91.6			1		24.1			5.4			66.8

Figure 3 :
Chart of percent inhibition by each molecule from the combinatorial library at 100 µM.

1500 diverse compounds against β-secretase using the computer program Maestro. A molecule was shown to bind in the active pocket of β-Secretase with a score of -9.73. This molecule was modeled as binding within the pocket using an Aspartate residue to hydrogen bond to the hydroxyl group of the molecule. This 2-propanol moiety within the molecule was used as a starting point to create a combinatorially library.

The library contained the epoxide opening products of 18 epoxides and 23 thiols, a possible 414 compounds. Of these 414 compounds 150 representative compounds were synthesize to test. All 150 compounds were tested at 100 µM endpoint, of these compounds 42 compounds demonstrated 50% inhibition or greater. These compounds were tested at 50 µM and 25 µM.

	Epoxide	Thiol	IC50 BACE1
1	Q	U”	10.66 µM ± 1.97 µM
2	S	T”	25.43 µM ± 6.08 µM
3	Q	T”	> 50µM
4	D	D”	10.46 µM ± 1.01 µM
5	L	W”	10.14 µM ± 1.06 µM
6	G	W”	16.85 µM ± 2.81 µM
7	S	D”	6.66 µM ± 1.01 µM
8	S	U”	12.59 µM ± 2.77 µM
9	A	Q”	36.05 µM ± 7.73 µM
10	N	L”	8.28 µM ± 0.78 µM
11	N	M”	11.00 µM ± 1.36 µM
12	A	M”	5.36 µM ± 0.38 µM
13	H	L”	7.52 µM ± 1.13 µM
14	Q	U”	9.60 µM ± 1.20 µM
15	A	D”	4.93 µM ± 0.86 µM
16	S	P”	7.09 µM ± 2.36 µM
17	N	B”	15.20 µM ± 1.36 µM

Figure 4: IC_{50} of Best from library

From these compounds the 17 that showed the best inhibition, **1-17** (Figure 4), were screened at multiple concentrations from 100 - 0.001 μM to determine the IC_{50} of the compounds. The compound with the best IC_{50} was then modified around the 2-propanol moiety to try and target the binding of the alcohol to the active aspartate residue in the bridge of the active site.

	Structure	IC_{50}
26	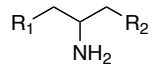	15.22 μM ± 4.72 μM
27	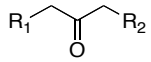	> 80 μM
28	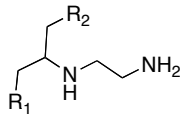	7.47 μM ± 0.83 μM
29	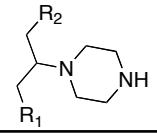	> 50 μM

Figure 5: Modifications altering hydrogen bonding of linker.

A variety of studies on the structure affinity relationship centering around the 2-propanol moiety. 17 modification were complete. The first study examined interaction with the enzymatic aspartate residue by modifying the alcohol to a better hydrogen donor, amine **26**, and then to a hydrogen bond acceptor, ketone **27**, and modifications on that, **28-29** (Figure 5). None of these modifications were able to display better activity than the starting point.

	Structure	IC_{50}
18	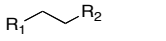	9.37 μM ± 1.21 μM
19	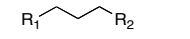	7.19 μM ± 0.60 μM
20	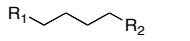	5.64 μM ± 0.43 μM
21	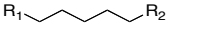	7.22 μM ± 0.84 μM
22	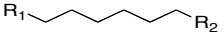	10.04 μM ± 2.69 μM

Figure 6: Modifications in linker length.

Since the modifications altering the hydrogen bonding ability showed no better improvement in binding affinity a second study examining the length of the carbon chain between the two aromatic groups was examined. The 2, 3, 4, 5, and 6 carbon linker were synthesized, **18-22** (Figure 6), and the IC_{50} were measured for each. The IC_{50} was shown to decrease from the 2-carbon to the 4-carbon and then begin to increase from the 5-carbon to the 6-carbon.

	Structure	IC_{50}
23	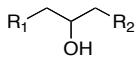	7.69 μM ± 0.90 μM
24	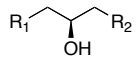	5.39 μM ± 0.81 μM
25	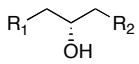	7.98 μM ± 1.02 μM

Figure 7: Effect of chirality on activity.

Third the effect on the chirality of the hydroxyl group was examined by synthesizing the enatiomerically pure S-enantiomer **24**, and R-enantiomer **25**. It was found that the S-entantiomer showed an decrease in IC50 while the R-enatiomer

stayed around the same value as the racemate. (Figure 7)

	Structure	IC_{50}
30	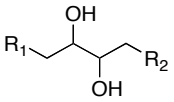	10.42 μM ± 1.45 μM
31	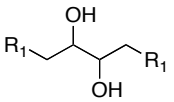	8.10 μM ± 1.78 μM
32	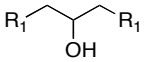	4.18 μM ± 0.98 μM
33	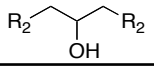	> 30 μM

Figure 8

With the information that the 4-carbon was the ideal length so a compound containing the 4-carbon linker with hydroxyl groups was synthesized, **30**, but no increase in binding affinity was observed experimentally. Seeing that the numerous changes in the linker were unable to break the IC_{50} threshold held by the original compound, the two dimers of the aromatic groups were made. The dimerization of the two carbazole groups, **32**, showed a much better inhibition than the dimer of the naphthalenethiol dimer, **33**, but only a slight increase in inhibition than the original compound **23**. The 4-carbon diol of the carbazole dimer was also synthesized, **31**, applying the ideal linker length found to the ideal side group found, but no increase in inhibition was observed.

Conclusions

In conclusion a new class of small molecule inhibitors was described and characterized. The structure activity relationship of the molecules has been investigated by varying both the side groups and the linker between the side groups in both size and functionality.

Methods

BACE1 Assay. Inhibition was determined using the Panvera BACE1 (β-Secretase) FRET Assay Kit, Red (P2985) sold by Invitrogen. In an opaque flat bottom 384 microtiter plate the inhibitor was diluted from 3 mM DMSO solution to the desired concentration in acetate Buffer so that no more than 10% DMSO existed in the sample. 10 μL of BACE1 substrate (3X solution, 750 nM) was plated into wells containing 10 μL of inhibitor at 3X concentration. 10 μL of β-Secretase enzyme solution (3X solution, 1.0 unit/mL) was added and the microtiter plate was let sit in the dark at room temperature. After 1 hour an endpoint reading was measured. This number was corrected from RFU to percent inhibition based on a Positive control (10% DMSO in Buffer, β-Secretase Substrate, and β-Secretase protein solution) representing 0% inhibition, and Negative control (10% DMSO in Buffer, β-Secretase Substrate) representing 100% inhibition. For IC50 determination the inhibitor is

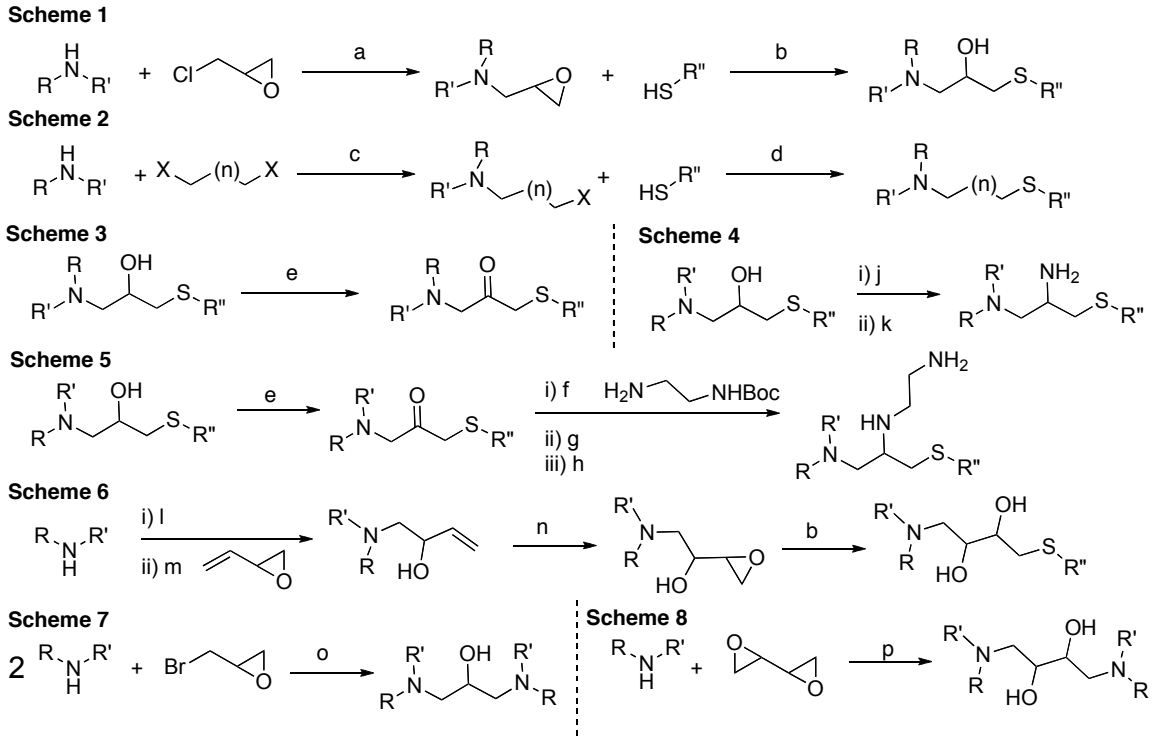

Figure 9 : Synthetic schemes used.
(a) KOH, $(Pr)_4NI$, RT, 2hr. (b) 9:1 EtOH:H_2O, reflux, 14 hr. (c) KOH, DMF, rt 16h. (d)K_2CO_3, DMF, rt ---> 85°C, 16h. (e) Dess.Martin Periodinone, dry DCM, 1h. (f) Acetic acid, MeOH, 2h. (g) $NaCHBH_3$ (h) 2M HCl in ether, 2h. (j)DCM, DMF, $SOCl_2$, 0°C ---> 45°C, 4h. (k) NH_3 (liq), DMF, -50°C ---> rt, 2 days. (l) NaH, DMF, 0°C ---> rt, 10 min. (m) 0°C, 3 hr. (n) mCPBA, DCM, $NaHCO_3$, 0°C ---> rt, 16h. (o) KOH, iPrOH, H_2O, reflux, 24h. (p) KO^tBu, ^tBuOH.

measured at multiple concentrations (100, 50, 10, 5, 1, 0.1, 0.01, 0.001μM) which are then corrected by the positive and negative controls and then fitted to the Hills plot and solved by using the program SigmaPlot®. If the measured Hill plot gave an error greater than 15 % the region in the plot where percent inhibition jumps sharply is expanded so that there are more points between the lowest and highest percent inhibition. If this did not yield a better curve then the inhibitor is diluted in less than 1% methanol instead of DMSO.

Synthesis. The majority of products, **1-17,** were produced by the nucleophilic epoxide opening reaction of an epoxide prepared by the substitution of epichlorohyrin, and a commercially available thiol (Scheme 1). Enantiomerically pure compounds, **24-25**, were synthesized through the use of enatiometrically pure epichlorohydrin in the epoxide opening (Scheme 1). Linker chain extensions, **18-22**, were prepared by the substitution of the dihalide of the linker with carbazole creating a monohalide, then substituted with the 2-naphthalenethiol (Scheme 2). It was observed that the reaction scheme 2 was highly dependent on the substrate. Different haloalkanes had to be used for different size chains, this was due to the elimination product of the dihalide being in competition with the

desired reaction. With smaller alkanes it was necessary to use the less reactive chloroalkane while this reacted too slow for the larger chains so the iodoalkane was used. The 2-carbon used the dichloroethane, the 3-carbon used the dibromopropane, and the 4-carbon used the diiodobutane. The 5 and 6 carbon chains were especially difficult, a 1-chloro-5-iodopentane (1-chloro-6-iodohexane) was used first to couple to the carbazole and then the chloro was replace by an iodine using NaI in acetone which was then reacted with the naphthalene thiol to produce 21 (and 22 respectively). The ketone, **27**, was produce by oxidation of compound **23** with the Dess Martin Periodinone (Scheme 3). Compounds **26** and **29** were produced by *in situ* substitution of the chlorinated compound **23** by scheme 4. **28** was synthesized by the epoxide opening of butadienemonooxide with carbazole and then the epoxidation of the produced alkene with mCPBA (Scheme 6). 31 was made using the double epoxide opening of 2,2'-bioxirane by carbazole (Scheme 8). Both **32** and **33** were made by substituting the epibromohydrin while opening the epoxide in simultaneously to create the dimers (Scheme 7).

Further Studies

To ensure that the best inhibitors found could be good drug molecules many more experiments must be completed. First of all the selectivity of the inhibitors must be established, this will be done by investigating the activity against similar proteases such as renin and Cathepsin D. Next the bioavailability must be modeled, this will be done by measuring the logD at multiple physiological pHs. To model the blood brain barrier the inhibitors will be subjected to a PAMPA (Parallel Artificial Membrain Permiabillity Assay). Lastly to help ensure good activity the inhibitors will be modeled via *in silico* methods.

References

(1) Venugopal, C.; Demos, C. M.; Jagannatha, K. S.; Pappolla, M. A.; Sambamurti, K. Beta-secretase: Structure, Function, and Evolution. *CNS Neurol Disord Drug Targets*. **2008**. 7(3). 278-294.

(2) Hu, X.; Hicks, C.W.; He, W.;Wong, P.; Maklin, W. B.; Trapp, B. D.; Yan, R. Bace1 modulates myelination in the central and peripheral nervous system. *Nature Neuro*. **2006**, 9, 1520 - 1525.

(3) Luo, X.; Yan, R. Inhibition of BACE1 for therapeutic use in Alzheimer's disease. *Int J Clin Exp Pathol.* **2010**. 3(6). 618-628.

(4) Bäck, M.; Nyhlén, J.; Kvarnström.; Appelgren, S.; Borkakoti, N.; Jansson, K.; Lindberg, J.; Nyström, S. Design, synthesis and SAR of potent statine-based BACE-1 inhibitors: Exploration of P1 phenoxy and benzyloxy residues. *Bioorg. Med. Chem.* **2008**. 16. 9471-9486.

(5) Malamas, M. S.; Erdei, J.; Gunawan, I.; Turner, J.; Hu, Y.; Wagner, E.; Fan, K.; Chopra, R.; Olland, A.; Bard, J.; Jacobsen, S. Design and Synthesis of 5,5'-Disubstituted Aminohydantoins as Potent and Selective Human β-Secretase

(BACE1) Inhibitors. *J. Med. Chem.* **2010**. 5. 1146-1158.

Original screening IC_{50} Compounds

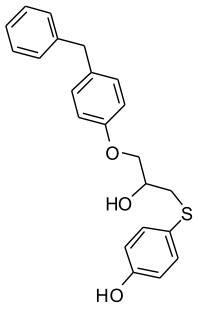

4-(3-(4-benzylphenoxy)-2-hydroxypropylthio)phenol (1) :
^{1}H NMR (400 MHz, $CDCl_3$): δ 7.33 – 7.23 (m, 4H), 7.21-7.16 (m, 3H), 7.08 (d, *J* = 8.5, 2H), 6.78 (d, *J* = 8.5, 2H), 6.70 (d, *J* = 8.6, 1H), 5.97 (s, 1H), 4.03-3.94 (m, 3H), 3.91 (s, 2H), 3.12 – 2.97 (m, 3H). **13C NMR (100 MHz, $CDCl_3$):** δC (ppm) 156.9, 155.9, 141.7, 134.1, 133.2, 130.2, 129.0, 128.7, 126.3, 124.9, 116.6, 114.8, 70.3, 68.9, 41.3, 39.7.

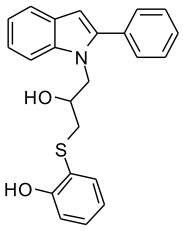

2-(2-hydroxy-3-(2-phenyl-1H-indol-1-yl)propylthio)phenol (2) : ^{1}H NMR (400 MHz, $CDCl_3$) δ 7.62 (d, *J* = 7.7 Hz, 1H), 7.46 – 7.33 (m, 6H), 7.30 – 7.19 (m, 3H), 7.15 (t, *J* = 7.4 Hz, 1H), 6.98 (s, 1H), 6.93 (d, *J* = 7.9 Hz, 1H), 6.81 (t, *J* = 7.5 Hz, 1H), 6.54 (s, 1H), 4.21 (qd, *J* = 14.8, 6.3 Hz, 2H), 3.85 (d, *J* = 2.7 Hz, 1H), 2.68 – 2.43 (m, *J* = 13.7, 6.0 Hz, 3H). **13C NMR (100 MHz, $CDCl_3$):** δC (ppm) 157.3, 141.6, 138.0, 136.2, 132.9, 131.6, 129.9, 128.9, 128.5, 122.3, 121.1, 120.9, 120.5, 118.6, 115.8, 110.6, 103.5, 69.5, 48.8, 41.1

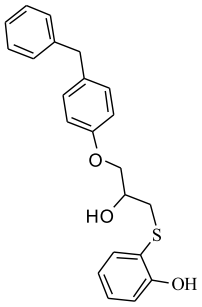

1-(4-benzylphenoxy)-3-(1-phenyl-1H-tetrazol-5-ylthio)propan-2-ol (3) :
^{1}H NMR (400 MHz, $CDCl_3$): δ 7.52 (dd, *J* = 7.7, 1.4, 1H), 7.36 – 7.16 (m, 6H), 7.10 (d, *J* = 8.5, 2H), 7.01 (d, *J* = 7.5, 1H), 6.87 (t, *J* = 7.5, 1H), 6.80 (d, *J* = 8.5, 2H), 4.06 – 3.88 (m, 6H), 3.11 (s, 1H), 3.00 (dd, *J* = 13.7, 4.3, 1H), 2.89 (dd, *J* = 13.7, 8.0, 1H). **13C NMR (100 MHz, $CDCl_3$):** δC (ppm)157.7, 156.9, 141.7, 136.6, 134.4, 131.7, 130.2, 129.1, 128.7, 126.3, 121.1, 118.7, 115.9, 114.8, 70.7, 68.8, 41.3, 40.1.

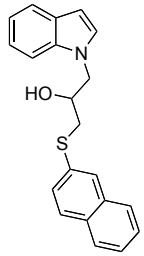

1-(1H-indol-1-yl)-3-(naphthalen-2-ylthio)propan-2-ol (4) :
^{1}H NMR (400 MHz, $CDCl_3$) δ 7.83 – 7.64 (m, 5H), 7.54 – 7.45 (m, 2H), 7.45 – 7.37 (m, 1H), 7.35 (d, *J* = 8.0, 1H), 7.25 – 7.10 (m, 3H), 6.55 (t, *J* = 6.3, 1H), 4.31 (dd, *J* = 14.2, 4.3, 1H), 4.12 (m, 2H), 3.10 (dd, *J* = 13.9, 4.9, 1H), 2.96 (dd, *J* = 13.9, 7.2, 1H), 2.81 – 2.16 (m, 1H). **13C NMR (100 MHz, $CDCl_3$):** δC (ppm) 136.4, 133.8, 132.2, 132.1, 128.9, 128.8, 128.7, 127.9, 126.9, 126.2, 121.9, 121.2, 119.8, 109.6, 101.9, 69.3, 50.8, 38.5.

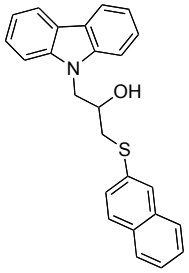

1-(9H-carbazol-9-yl)-3-(naphthalen-2-ylthio)propan-2-ol (23) .
^{1}H NMR (400 MHz, $CDCl_3$) δ 8.12 – 8.06 (m, 2H), 7.79 – 7.71 (m, 1H), 7.69 (d, *J* = 8.5 Hz, 1H), 7.61 (s, 1H), 7.55 – 7.31 (m, 8H), 7.29 - 7.23 (m, 2H), 4.51 – 4.42 (m, 1H), 4.42 – 4.34 (m, 1H), 4.29 (s, 1H), 3.21 - 3.16 (m, 1H), 3.11 – 3.00 (m, 1H), 2.57 (s, 1H).13C NMR (100 MHz, $CDCl_3$): δC (ppm) 140.9, 133.8, 132.3, 132.1, 128.9, 127.8, 127.7, 127.4, 127.3, 126.8, 126.2, 126.1, 123.2, 120.5, 119.5, 109.2, 69.2, 48.0, 38.8

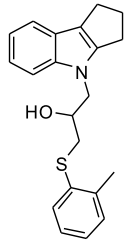

1-(2,3-dihydrocyclopenta[b]indol-4(1H)-yl)-3-(o-tolylthio)propan-2-ol (5) : ^{1}H NMR (400 MHz, $CDCl_3$) δ 7.46 (d, *J* = 6.7 Hz, 1H), 7.27 (d, *J* = 7.4 Hz, 1H), 7.18 (dd, *J* = 14.2, 6.2 Hz, 2H), 7.15 – 7.07 (m, 4H), 4.21 (dd, *J* = 16.7, 7.4 Hz, 1H), 4.10 (t, *J* = 8.2 Hz, 2H), 3.07 – 3.00 (m, 1H), 2.93 (d, *J* = 6.5 Hz, 1H), 2.87 (dd, *J* = 14.1, 7.2 Hz, 4H), 2.55 (dd, *J* = 13.4, 6.8 Hz, 2H), 2.46 – 2.37 (m, 4H). **13C NMR (101 MHz, $CDCl_3$):** δC (ppm) 146.5, 141.3, 138.3, 134.2, 130.6, 128.9, 126.7, 126.6, 124.8, 120.4, 119.5, 118.8, 118.6, 109.9, 69.5, 49.6, 38.1, 28.5, 25.6, 24.8, 20.6.

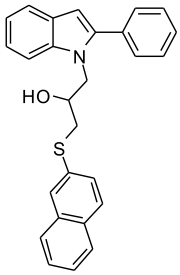

1-(naphthalen-2-ylthio)-3-(2-phenyl-1H-indol-1-yl)propan-2-ol (7) : ^{1}H NMR (400 MHz, $CDCl_3$) δ 7.83 – 7.76 (m, 1H), 7.72 – 7.65 (m, 2H), 7.64 – 7.57 (m, 1H), 7.54 – 7.34 (m, 9H), 7.27 – 7.15 (m, 3H), 6.59 (s, 1H), 4.40 – 4.35 (m, 2H), 4.04-3.99 (m, 1H), 2.88 (dd, *J* = 14.0, 4.2 Hz, 1H), 2.74 (dd, *J* = 14.0, 8.2 Hz, 1H), 2.38 (d, *J* = 3.6 Hz, 1H). **13C NMR (100 MHz, $CDCl_3$):** δC (ppm) 141.7, 138.0, 133.9, 133.0, 132.4, 132.2, 129.9, 128.9, 128.9, 128.5, 128.4, 127.9, 127.7, 127.5, 127.4, 126.9, 126.2, 122.3, 120.1, 120.5, 110.7, 103.5, 69.0, 48.7, 38.9

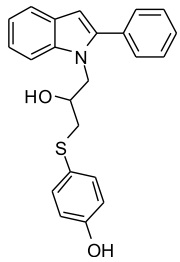

4-(2-hydroxy-3-(2-phenyl-1H-indol-1-yl)propylthio)phenol (8) : ^{1}H NMR (400 MHz, $CDCl_3$) δ 7.61 (d, *J* = 7.7 Hz, 1H), 7.48 – 7.32 (m, 6H), 7.27 – 7.09 (m, *J* = 24.2, 17.4, 10.3 Hz, 2H), 7.03 (d, *J* = 8.6 Hz, 2H), 6.61 (d, *J* = 8.6 Hz, 2H), 6.52 (s, 1H), 5.42 (s, 1H), 4.29 (d, *J* = 6.3 Hz, 2H), 3.85 (s, 1H), 2.60 (qd, *J* = 13.9, 6.2 Hz, 2H), 2.46 – 2.33 (m, *J* = 2.0 Hz, 1H). **13C NMR (100 MHz, $CDCl_3$):** δC (ppm) 155.6, 141.7, 138.0, 133.8, 133.0, 129.9, 128.8, 128.4, 128.3, 124.8, 122.1, 120.9, 120.4, 116.5, 110.6, 103.3, 69.1, 48.6, 41.0

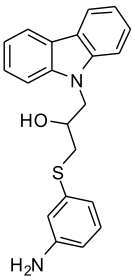

1-(3-aminophenylthio)-3-(9H-carbazol-9-yl)propan-2-ol (9) :
^{1}H NMR (400 MHz, $CDCl_3$) δ 8.09 (d, *J* = 7.7 Hz, 2H), 7.50 – 7.38 (m, 4H), 7.26 - 7.21 (m, 2H), 6.97 (t, *J* = 7.8 Hz, 1H), 6.64 (d, *J* = 7.7 Hz, 1H), 6.45 – 6.31 (m, 2H), 4.45 (dd, *J* = 14.9, 5.6 Hz, 1H), 4.38 (dd, *J* = 14.9, 6.5 Hz, 1H), 4.32 – 4.18 (m, 1H), 3.38 (s, 1H), 3.04 (dd, *J* = 14.0, 4.7 Hz, 1H), 2.91 (dd, *J* = 14.0, 7.5 Hz, 1H), 2.66 (s, 1H). **13C NMR (100 MHz, $CDCl_3$):** 147.2, 140.9, 135.7, 130.1, 126.1, 123.2, 120.5, 119.5, 115.3, 113.6, 109.3, 69.2, 47.9, 38.7.

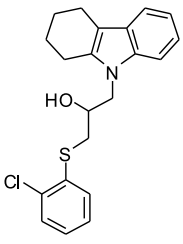

1-(2-chlorophenylthio)-3-(3,4-dihydro-1H-carbazol-9(2H)-yl)propan-2-ol (10) : ^{1}H NMR (400 MHz, $CDCl_3$) δ 7.48 (d, *J* = 7.3 Hz, 0H), 7.41 – 7.35 (m, 0H), 7.26 (d, *J* = 7.7 Hz, 0H), 7.17 – 7.06 (m, 2H), 4.25 – 4.01 (m, 3H), 3.08 (dd, *J* = 13.7, 4.3 Hz, 1H), 2.96 (dd, *J* = 13.7, 7.2 Hz, 1H), 2.82 – 2.59 (m, 4H), 2.44 (d, *J* = 3.2 Hz, 1H), 2.00 – 1.79 (m, 4H). **13C NMR (100 MHz, $CDCl_3$):** δC (ppm) 136.7, 135.9, 134.6, 134.5, 130.2, 129.7, 127.8, 127.6, 127.5, 121.1, 119.3, 118.2, 110.4, 109.2, 69.6, 47.9, 38.0, 23.5, 23.4, 22.7, 21

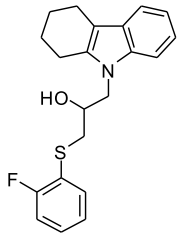

1-(3,4-dihydro-1H-carbazol-9(2H)-yl)-3-(2-fluorophenylthio)propan-2-ol (11) : ^{1}H NMR (400 MHz, $CDCl_3$) δ 7.47 (d, *J* = 7.6 Hz, 0H), 7.33 (t, *J* = 7.6 Hz, 0H), 7.26 (t, *J* = 8.2 Hz, 1H), 7.17 – 7.02 (m, 1H), 4.19 (dd, *J* = 13.8, 3.6 Hz, 1H), 4.06 (dd, *J* = 21.7, 7.9 Hz, 2H), 3.11 – 3.02 (m, *J* = 9.5, 4.9 Hz, 1H), 2.94 (dd, *J* = 13.6, 7.1 Hz, 1H), 2.81 – 2.60 (m, 4H), 2.44 (s, 1H), 2.00 – 1.81 (m, 4H). **13C NMR (100 MHz, $CDCl_3$):** δC (ppm) 136.7, 136.0, 133.0, 129.6, 129.4, 127.8, 125.0, 121.0, 119.2, 118.1, 116.3, 116.1, 110.3, 109.2, 69.9, 47.8, 38.8, 23.5, 23.4, 22.7, 21.3.

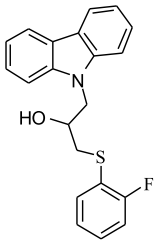

1-(9H-carbazol-9-yl)-3-(2-fluorophenylthio)propan-2-ol (12) :
^{1}H NMR (400 MHz, $CDCl_3$) δ 8.07 (d, *J* = 7.7, 2H), 7.43 (d, *J* = 3.3, 4H), 7.32 (t, *J* = 7.5, 1H), 7.28 – 7.18 (m, 3H), 7.10 – 6.96 (m, 2H), 4.49 (dd, *J* = 15.0, 4.5, 1H), 4.40 (dd, *J* = 15.0, 6.8, 1H), 4.19 (m, 1H), 3.13 (dd, *J* = 13.7, 4.7, 1H), 2.99 (dd, *J* = 13.7, 7.5, 1H), 2.44 (s, 1H). **13C NMR (100 MHz, $CDCl_3$):** δC (ppm) 141.0, 133.4, 129.7, 129.6, 126.1, 124.9, 123.2, 120.5, 119.6, 116.3, 116.1, 109.2, 69.6, 48.0, 39.22.

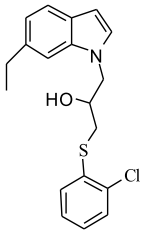

1-(2-chlorophenylthio)-3-(6-ethyl-1H-indol-1-yl)propan-2-ol (13) :
^{1}H NMR (400 MHz, $CDCl_3$): δ 7.49 (d, *J* = 7.7, 1H), 7.38 (d, *J* = 7.5, 1H), 7.14 – 6.97 (m, 6H), 6.52 (d, *J* = 2.8, 1H), 4.50 (dd, *J* = 14.8, 4.5, 1H), 4.29 (dd, *J* = 14.8, 7.6, 1H), 4.00 (m, 1H), 3.05 – 2.90 (m, 4H), 2.44 (d, *J* = 3.5, 1H), 1.33 – 1.26 (m, 3H). **13C NMR (100 MHz, $CDCl_3$):** δC (ppm) 134.4, 134.3, 134.1, 130.6, 130.2, 129.5, 127.6, 123.2, 120.4, 119.5, 102.7, 70.4, 53.7, 37.5, 26.0, 15.9.

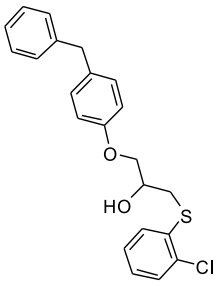

1-(4-benzylphenoxy)-3-(2-chlorophenylthio)propan-2-ol (14) :
^{1}H NMR (400 MHz, $CDCl_3$): δ 7.38 (dd, *J* = 14.7, 7.8, 2H), 7.30 – 7.23 (m, 2H), 7.21 – 7.12 (m, 4H), 7.09 (d, *J* = 7.6, 3H), 6.82 (t, *J* = 9.4, 2H), 4.17 – 3.95 (m, 3H), 3.92 (s, 2H), 3.27 (dd, *J* = 13.7, 5.4, 1H), 3.15 (dd, *J* = 13.6, 6.7, 1H), 2.74 (s, 1H). **13C NMR (100 MHz, $CDCl_3$):** δC (ppm) 157.2, 156.9, 141.7, 134.7, 134.6, 134.2, 130.2, 130.0, 129.0, 128.7, 127.6, 127.5, 126.2, 114.8, 70.4, 68.8, 41.2, 36.7.

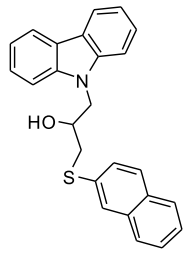

1-(9H-carbazol-9-yl)-3-(naphthalen-2-ylthio)propan-2-ol (15) :
^{1}H NMR (400 MHz, $CDCl_3$): δ 8.11 (d, *J* = 7.7, 2H), 7.76 (d, *J* = 7.9, 1H), 7.69 (d, *J* = 8.6, 1H), 7.62 (s, 1H), 7.56 – 7.33 (m, 8H), 7.26 (m, 2H), 4.47 (dd, *J* = 14.9, 5.0, 1H), 4.38 (dd, *J* = 14.8, 6.7, 1H), 4.33 – 4.25 (m, 1H), 3.18 (dd, *J* = 13.9, 4.7, 1H), 3.06 (dd, *J* = 13.8, 7.3, 1H), 2.73 – 2.44 (m, 1H). **13C NMR (100 MHz, $CDCl_3$):** δC (ppm) 141.0, 133.9, 132.4, 132.2, 129.0, 127.9, 127.8, 127.5, 127.4, 126.9, 126.3, 126.2, 123.3, 120.6, 119.6, 109.3, 69.3, 48.1, 38.9.

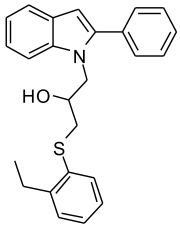

1-(2-ethylphenylthio)-3-(2-phenyl-1H-indol-1-yl)propan-2-ol (16) : ^{1}H NMR (400 MHz, $CDCl_3$) δ 7.68 (d, *J* = 7.7 Hz, 0H), 7.56 – 7.38 (m, 2H), 7.31 – 7.12 (m, 1H), 7.10 – 7.01 (m, 0H), 6.95 (d, *J* = 7.8 Hz, 0H), 6.61 (s, 0H), 4.40 – 4.33 (m, 2H), 4.07 – 3.95 (m, 1H), 2.84 – 2.63 (m, 4H), 2.35 (d, *J* = 3.5 Hz, 1H), 1.23 (t, *J* = 7.5 Hz, 3H). **13C NMR (100 MHz, $CDCl_3$):** δC (ppm) 144.1, 141.8, 138.1, 133.7, 133.1, 130.0, 129.0, 128.9, 128.5, 128.4, 126.8, 126.8,122.2, 121.0, 120.5, 110.8, 103.5, 69.13, 48.8, 38.6, 27.1, 15.0

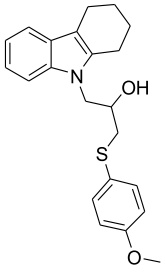

1-(3,4-dihydro-1H-carbazol-9(2H)-yl)-3-(4-methoxyphenylthio)propan-2-ol (17) : ^{1}H NMR (400 MHz, $CDCl_3$) δ 7.45 (d, *J* = 7.3, 1H), 7.31 (d, *J* = 8.7, 2H), 7.26 – 7.20 (m, 1H), 7.12-7.04 (m, 2H), 6.81 (d, *J* = 8.7, 2H), 4.21 – 4.10 (m, 1H), 4.07-4.00 (m, 2H), 3.78 (s, 3H), 2.97 (dd, *J* = 13.7, 4.5, 1H), 2.85 (dd, *J* = 13.7, 7.3, 1H), 2.78 – 2.58 (m, 4H), 2.46 (s, 1H), 1.97 – 1.78 (m, 4H). **13C NMR (100 MHz, $CDCl_3$):** δC (ppm)159.6, 136.7, 136.0, 133.7, 127.7, 125.1, 121.0, 119.2, 118.0, 115.1, 110.2, 109.2, 69.6, 55.6, 47.8, 41.1, 23.5, 23.4, 22.7, 21.3.

Modification of Combinatorial Library

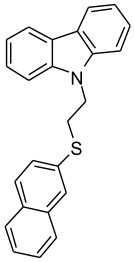

9-(2-(naphthalen-2-ylthio)ethyl)-9H-carbazole (18) :
^{1}H NMR (400 MHz, $CDCl_3$) δ 8.08 – 8.02 (m, 2H), 7.83-7.72 (m, 4H), 7.54 – 7.39 (m, 5H), 7.31 – 7.20 (m, 4H), 4.56 – 4.49 (m, 2H), 3.43 – 3.36 (m, 2H). 13C NMR (100 MHz, $CDCl_3$): δC (ppm) 140.0, 133.7, 132.2, 132.1, 128.7, 128.0, 127.8, 127.5, 127.1, 126.7, 126.0, 125.7, 123.0, 120.4, 119.2, 108.4, 42.5, 31.8.

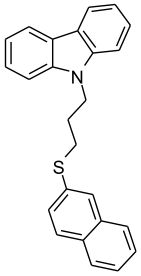

9-(3-(naphthalen-2-ylthio)propyl)-9H-carbazole (19) :
^{1}H NMR (400 MHz, $CDCl_3$) δ 8.19 – 8.13 (m, 2H), 7.82 – 7.77 (m, 1H), 7.74 (dd, *J* = 8.5, 3.8 Hz, 1H), 7.70 – 7.60 (m, 2H), 7.52 – 7.38 (m, 7H), 7.32 – 7.26 (m, 2H), 4.49 - 4.46 (m, 2H), 3.03 – 2.97 (m, 2H), 2.30 – 2.22 (m, 2H). 13C NMR (100 MHz, $CDCl_3$): δC (ppm) 140.4, 133.8, 133.2, 131.8, 128.6, 127.7, 127.4, 127.2, 127.1, 126.6, 125.8, 125.8, 123.0, 120.5, 119.1, 108.7, 41.3, 30.8, 28.1.

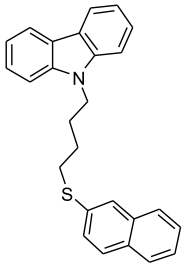

9-(4-(naphthalen-2-ylthio)butyl)-9H-carbazole (20) :
^{1}H NMR (400 MHz, $CDCl_3$) δ 8.13 (dd, *J* = 7.8, 0.7 Hz, 2H), 7.84 – 7.79 (m, 1H), 7.73 (dd, *J* = 6.1, 5.6 Hz, 2H), 7.53 – 7.44 (m, 3H), 7.42 – 7.36 (m, 2H), 7.31 – 7.23 (m, 2H), 4.29 (t, *J* = 7.1 Hz, 2H), 2.99 (t, *J* = 7.1 Hz, 2H), 2.12 – 2.01 (m, 2H), 1.79 - 1.72 (m, 2H). 13C NMR (100 MHz, $CDCl_3$): δC (ppm) 140.5, 133.9, 133.9, 131.9, 128.6, 127.9, 127.7, 127.4, 127.2, 126.7, 125.8, 125.8, 123.0, 120.5, 119.0, 108.7, 42.7, 33.6, 28.1, 26.8.

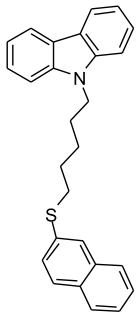

9-(5-(naphthalen-2-ylthio)pentyl)-9H-carbazole (21) :
^{1}H NMR (400 MHz, cdcl$_3$) δ 8.16 (d, *J* = 7.8 Hz, 2H), 7.83 – 7.73 (m, 4H), 7.53 – 7.38 (m, 7H), 7.32 – 7.25 (m, 2H), 4.28 (t, *J* = 7.1 Hz, 2H), 2.97 (t, *J* = 10.3, 2H), 1.94 – 1.85 (m, 2H), 1.79 – 1.67 (m, 2H), 1.59 – 1.48 (m, 2H). 13C NMR (100 MHz, CDCl$_3$): δC (ppm) 140.5, 134.3, 133.9, 131.8, 128.5, 127.9, 127.4, 127.2, 126.8, 126.7, 125.8, 125.7, 123.0, 120.5, 119.0, 108.8, 42.9, 33.4, 29.1, 28.7, 26.6.

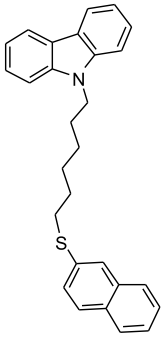

9-(6-(naphthalen-2-ylthio)hexyl)-9H-carbazole (22) :
^{1}H NMR (400 MHz, cdcl$_3$) δ 8.14 (dd, *J* = 7.7, 0.6 Hz, 2H), 7.82 – 7.71 (m, 4H), 7.51 – 7.37 (m, 7H), 7.29 – 7.24 (m, 2H), 4.28 (t, *J* = 7.1 Hz, 2H), 2.98 (t, *J* = 7.2 Hz, 2H), 1.91 - 1.84 (m, 2H), 1.72 – 1.63 (m, 2H), 1.54 – 1.45 (m, 2H), 1.43 - 1.36 (m, 2H). 13C NMR (100 MHz, CDCl$_3$): δC (ppm) 140.6, 135.6, 134.0, 131.8, 128.5, 127.9, 127.3, 127.1, 126.7, 126.5, 125.8, 125.7, 123.0, 120.5, 118.9, 108.8, 43.0, 33.5, 29.1, 29.0, 28.7, 27.0.

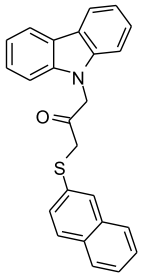

1-(9H-carbazol-9-yl)-3-(naphthalen-2-ylthio)propan-2-one (27) :
^{1}H NMR (400 MHz, cdcl$_3$) δ 8.10 – 8.06 (m, 2H), 7.81 – 7.68 (m, 4H), 7.52 – 7.45 (m, 2H), 7.39 – 7.33 (m, 3H), 7.27 - 7.23 (m, 2H), 7.13 (d, *J* = 8.2 Hz, 2H), 5.12 (s, 2H), 3.66 (s, 2H). 13C NMR (100 MHz, CDCl$_3$): δC (ppm) 200.6, 140.5, 133.8, 132.4, 131.4, 129.2, 128.8, 127.9, 127.5, 127.5, 127.0, 126.5, 126.2, 123.4, 120.7, 120.0, 108.5, 50.8, 40.8.

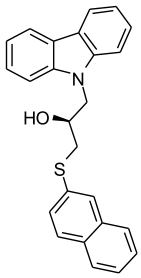

(S)-1-(9H-carbazol-9-yl)-3-(naphthalen-2-ylthio)propan-2-ol (24) .
^{1}H NMR (400 MHz, CDCl$_3$) δ 8.10 - 8.07 (m, 2H), 7.77 – 7.66 (m, 2H), 7.62 (s, 1H), 7.54 – 7.48 (m, 1H), 7.47 – 7.33 (m, 7H), 7.25 - 7.21 (m, 2H), 4.52 (dd, *J* = 14.9, 5.3 Hz, 1H), 4.47 – 4.39 (m, 1H), 4.32 (s, 1H), 3.25 - 3.19 (m, 1H), 3.12 – 3.04 (m, 1H), 2.47 (d, *J* = 3.6 Hz, 1H). 13C NMR (100 MHz, CDCl$_3$): δC (ppm) 140.9, 133.9, 132.3, 132.2, 129.0, 127.9, 127.8, 127.5, 127.4, 126.9, 126.3, 126.1, 123.3, 120.6, 119.6, 109.2, 69.2, 48.0, 39.0.

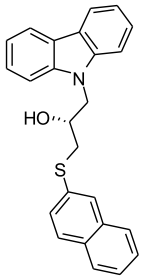

(R)-1-(9H-carbazol-9-yl)-3-(naphthalen-2-ylthio)propan-2-ol (25) .
^{1}H NMR (400 MHz, CDCl$_3$) δ 8.11 – 8.07 (m, 2H), 7.77 – 7.72 (m, 1H), 7.69 (d, *J* = 8.8 Hz, 1H), 7.62 (d, *J* = 1.4 Hz, 1H), 7.54 – 7.49 (m, 1H), 7.46 – 7.34 (m, 7H), 7.25 - 7.21 (m, 2H), 4.52 (dd, *J* = 14.9, 5.4 Hz, 1H), 4.43 (dd, *J* = 14.9, 6.6 Hz, 1H), 4.32 (s, 1H), 3.22 (dd, *J* = 13.9, 4.8 Hz, 1H), 3.09 (dd, *J* = 14.0, 7.5 Hz, 1H), 2.46 (d, *J* = 2.9 Hz, 1H). 13C NMR (100 MHz, CDCl$_3$): δC (ppm) 140.9, 133.9, 132.2, 132.2, 129.0, 127.9, 127.6, 127.4, 126.9, 126.3, 126.1, 123.3, 120.6, 119.6, 109.2, 69.2, 48.0, 39.1.

Supporting Information of BACE1 Assay

1 IC_{50} = 10.66 μM ± 1.97 μM

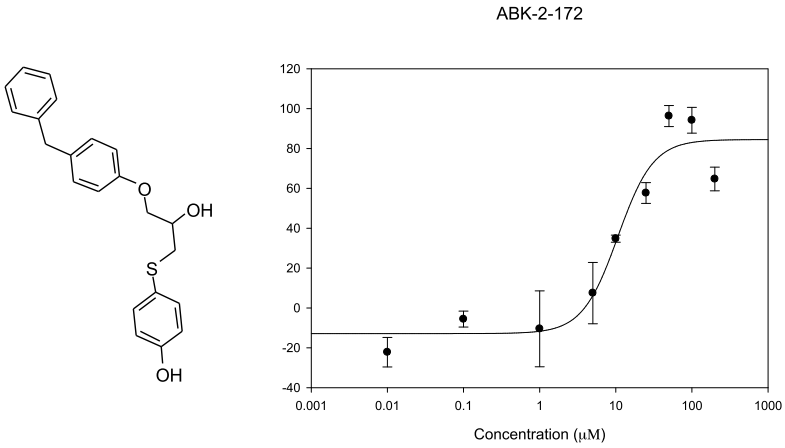

2 IC_{50} = 25.43 μM ± 6.08 μM

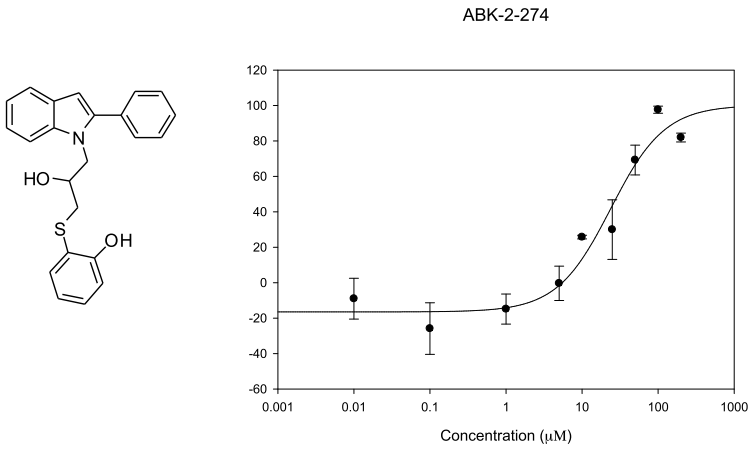

4 IC_{50} = 10.46 μM ± 0.88 μM

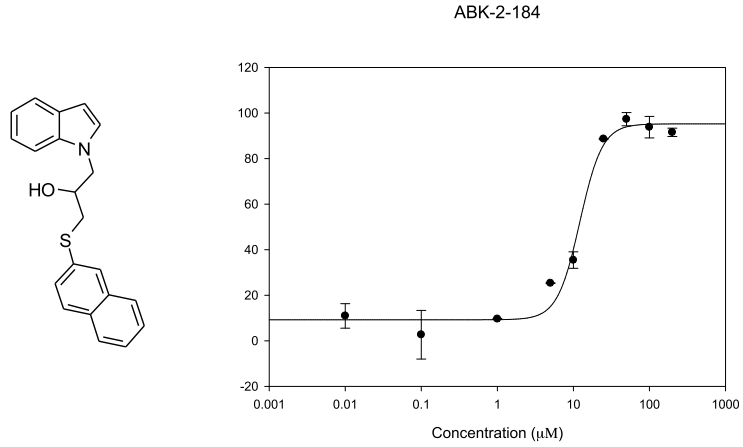

5 $IC_{50} = 10.14\ \mu M \pm 1.06\ \mu M$

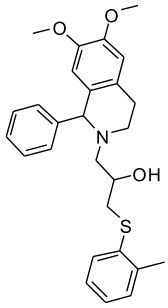

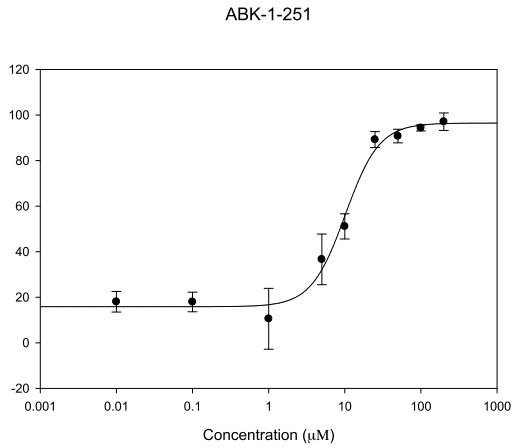

6 $IC_{50} = 16.85\ \mu M \pm 2.81\ \mu M$

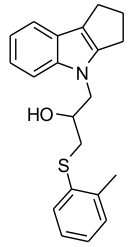

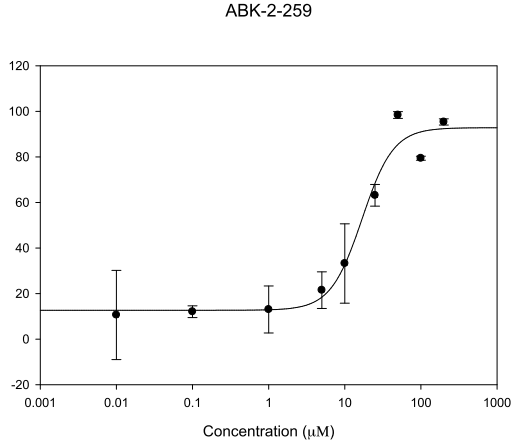

7 $IC_{50} = 6.66\ \mu M \pm 1.01\ \mu M$

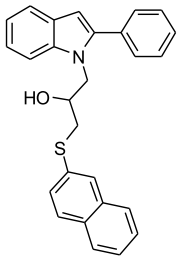

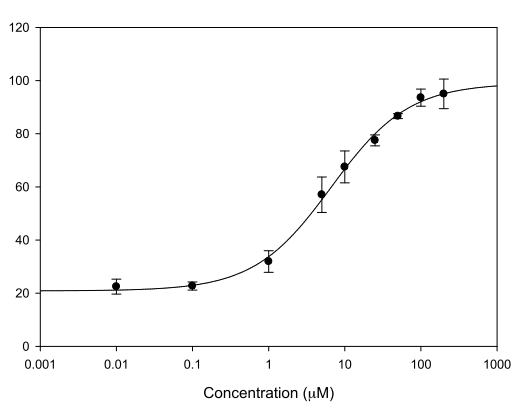

8 $IC_{50} = 12.59\ \mu M \pm 2.77\ \mu M$

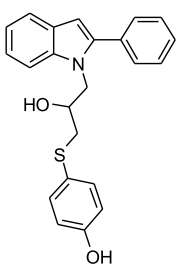

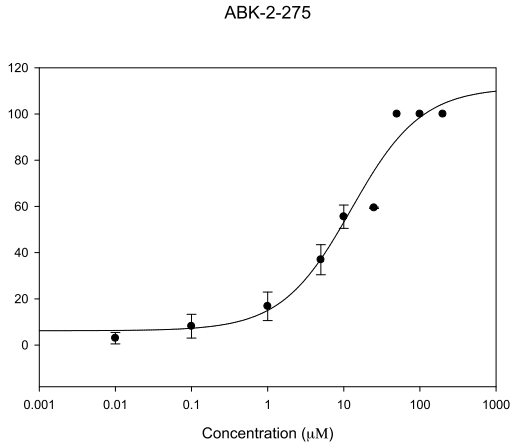

9 $IC_{50} = 36.05\ \mu M \pm 7.73\ \mu M$

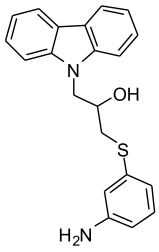

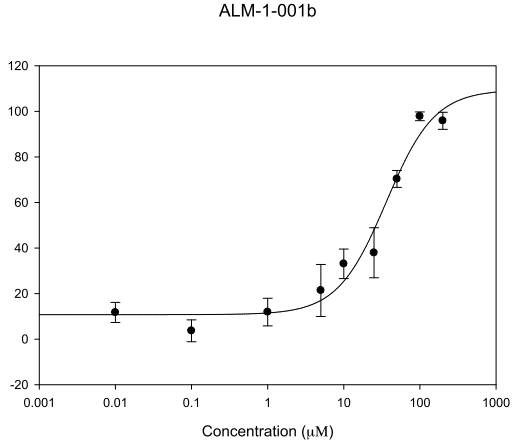

10 $IC_{50} = 8.28\ \mu M \pm 0.78\ \mu M$

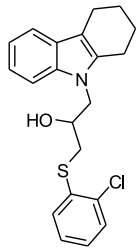

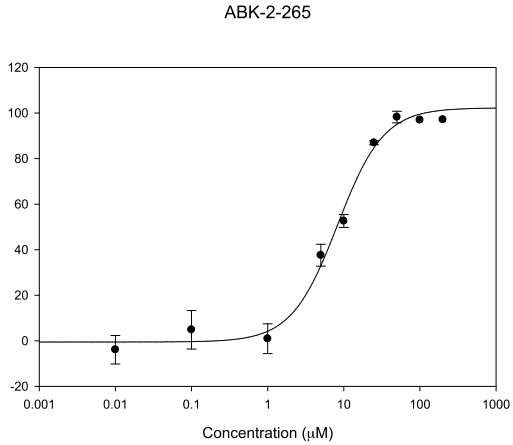

11 IC_{50} = 11.00 μM ± 1.36 μM

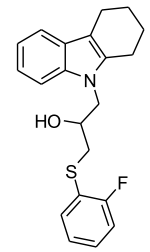

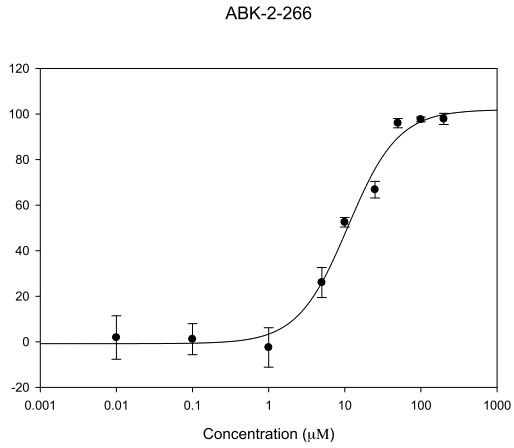

12 IC_{50} = 5.36 μM ± 0.38 μM

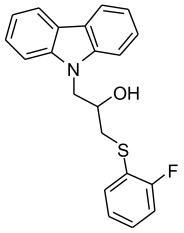

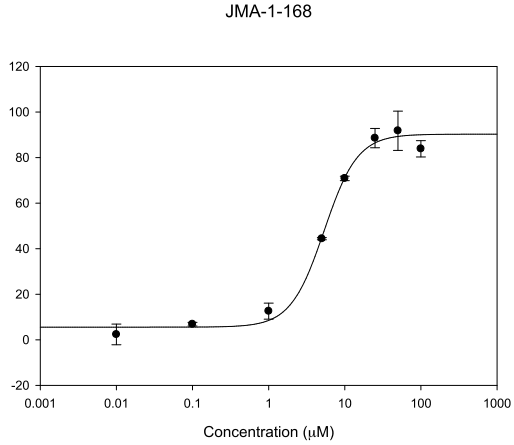

13 IC_{50} = 7.52 μM ± 1.13 μM

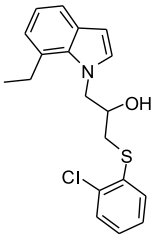

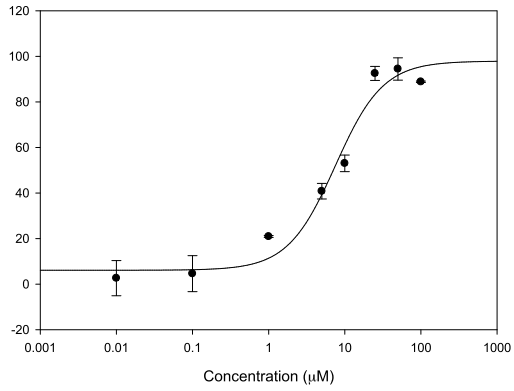

14 $IC_{50} = 9.60\ \mu M \pm 1.20\ \mu M$

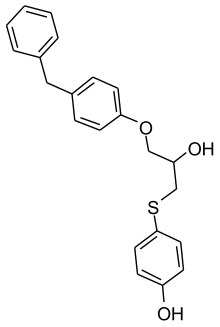

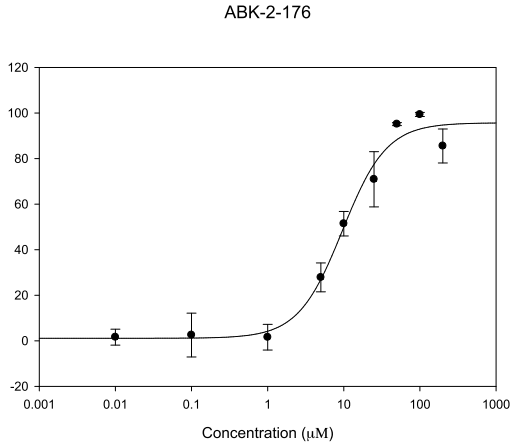

15 $IC_{50} = 4.93\ \mu M \pm 0.86\ \mu M$

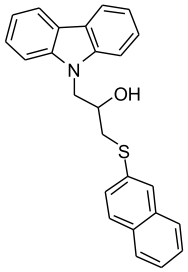

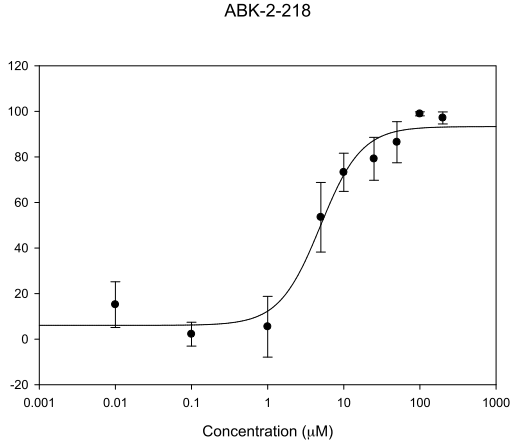

16 $IC_{50} = 7.09\ \mu M \pm 2.36\ \mu M$

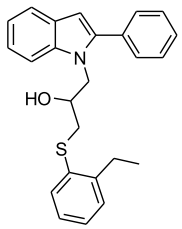

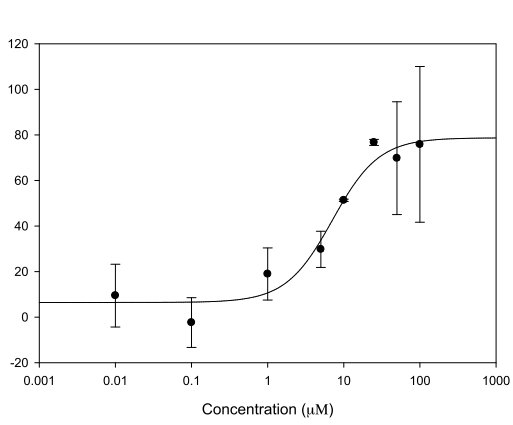

17 IC_{50} = 15.20 μM ± 1.36 μM

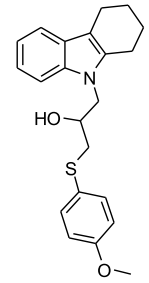

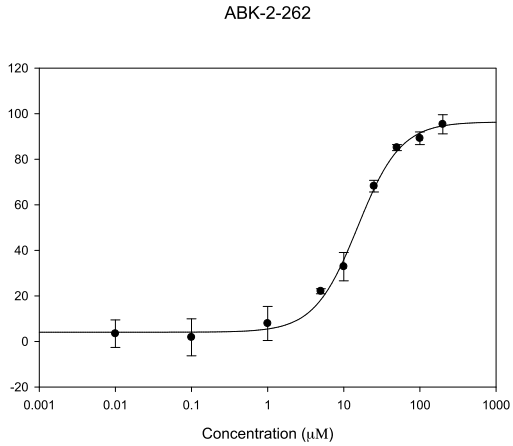

Modifications

Modifications from original combinatorial library. Compounds (18-32)

32 IC_{50} = 4.18 μM ± 0.98 μM

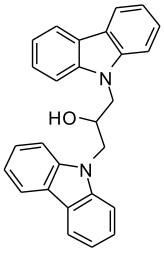

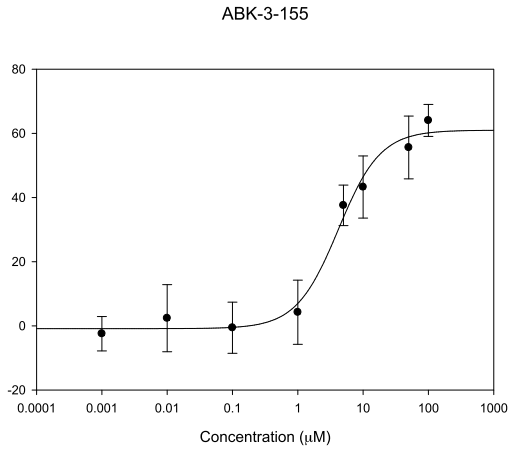

18 $IC_{50} = 9.37\ \mu M \pm 1.21\ \mu M$

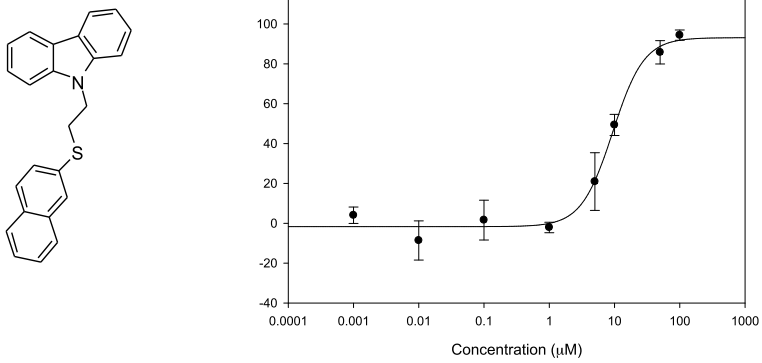

19 $IC_{50} = 7.19\ \mu M \pm 0.60\ \mu M$

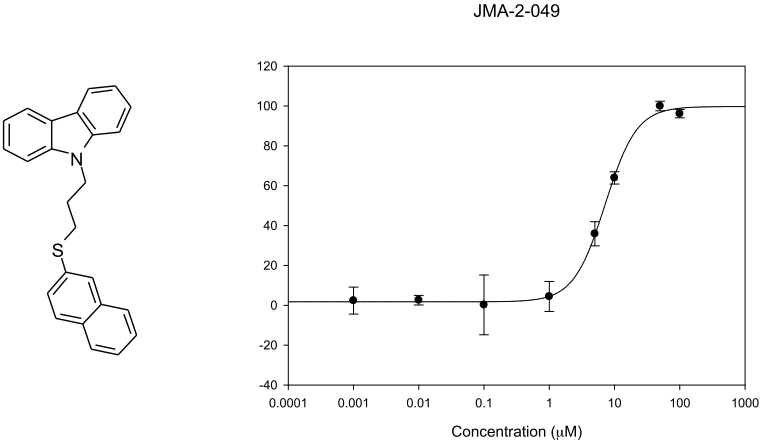

20 $IC_{50} = 5.64\ \mu M \pm 0.43\ \mu M$

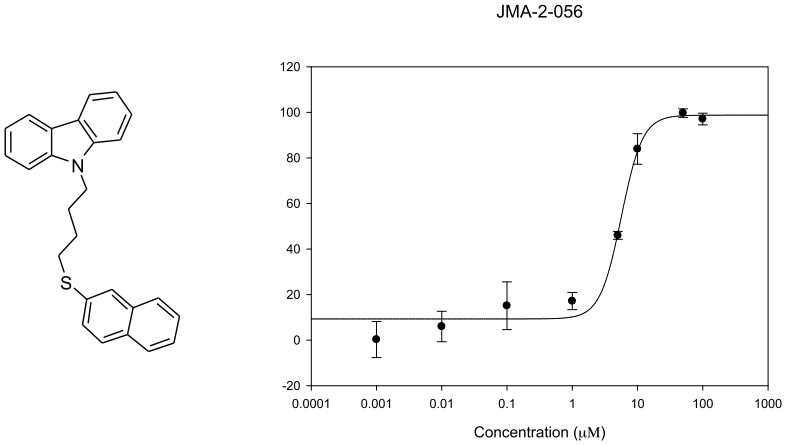

21 IC_{50} = 7.22 μM ± 0.84 μM

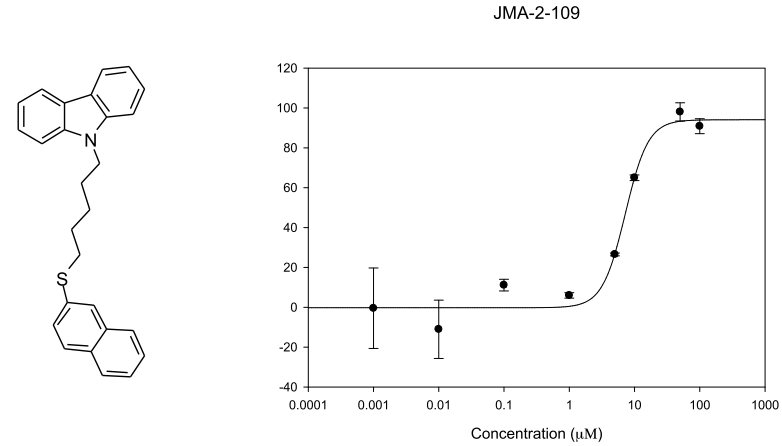

22 IC_{50} = 10.04 μM ± 2.69 μM

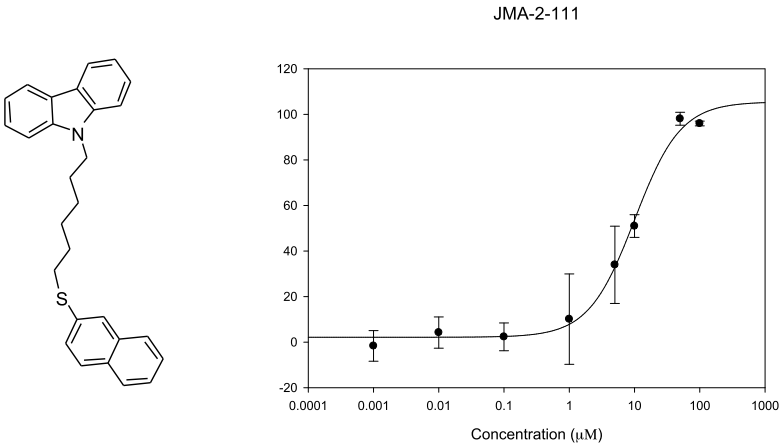

24 IC_{50} = 5.39 μM ± 0.81 μM

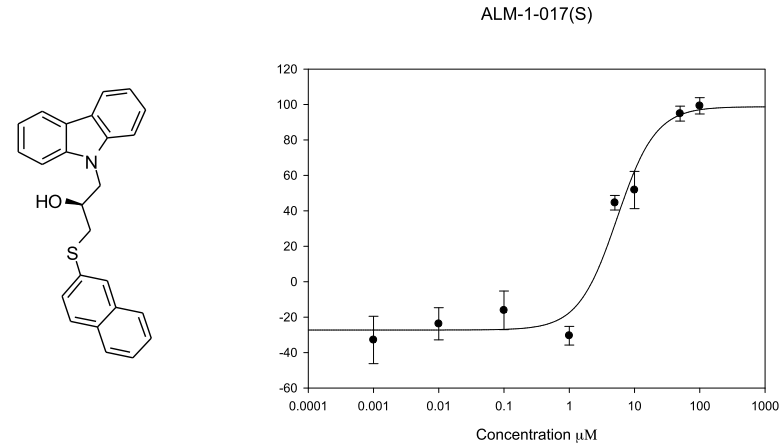

25 IC_{50} = 7.98 μM ± 1.02 μM

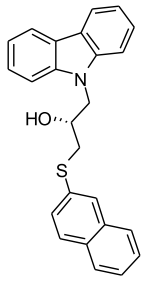

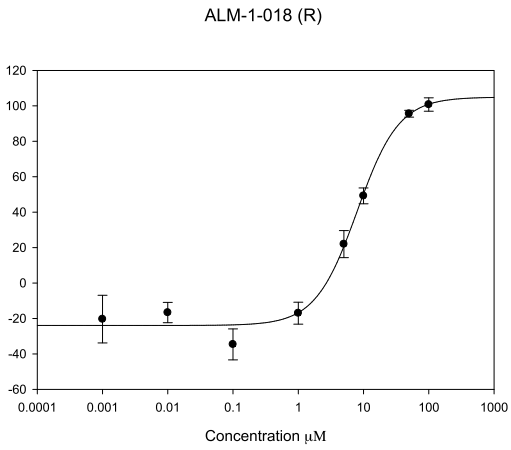

31 IC_{50} = 8.10 μM ± 1.78 μM

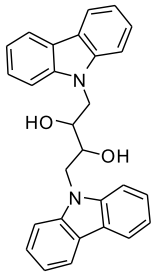

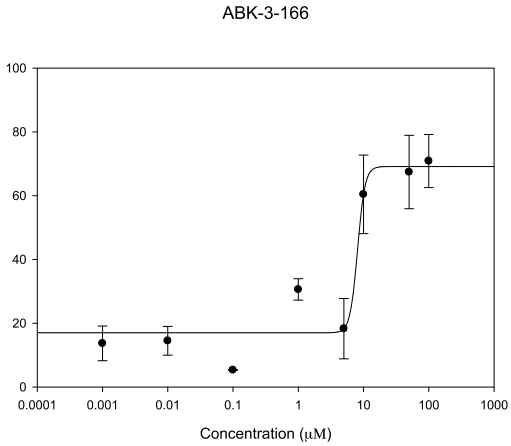

23 IC_{50} = 7.69 μM ± 0.90 μM

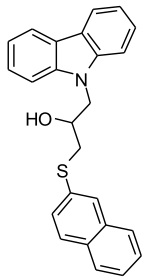

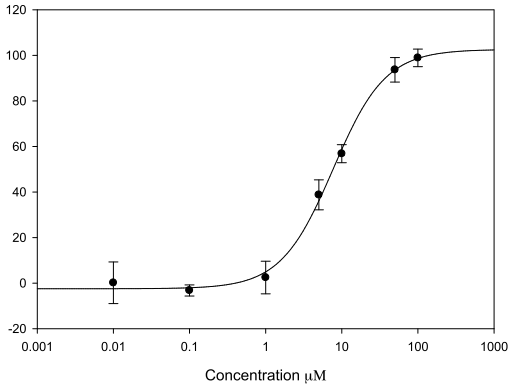

30 IC_{50} = 10.42 μM ± 1.45 μM

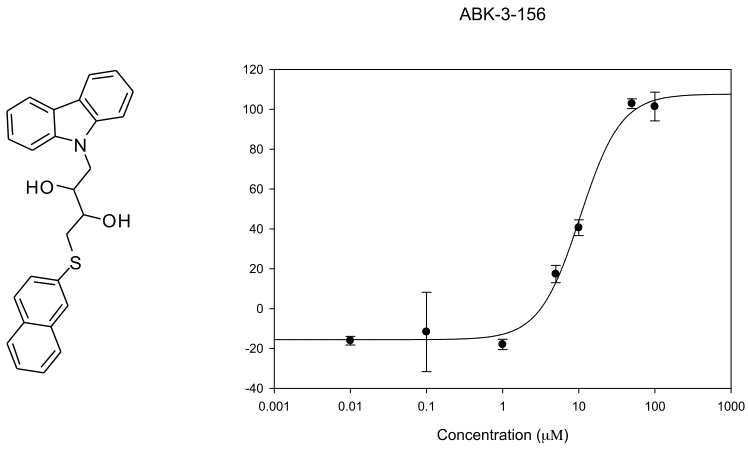

28 IC_{50} = 7.47 μM ± 0.83 μM

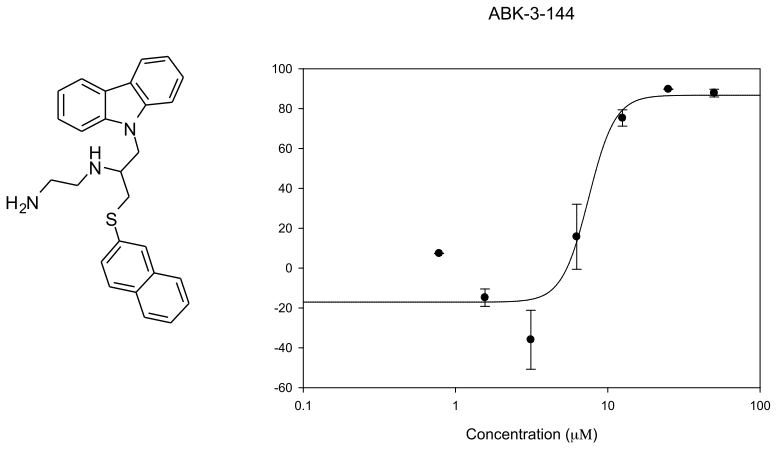

26 IC_{50} = 15.22 μM ± 4.72 μM

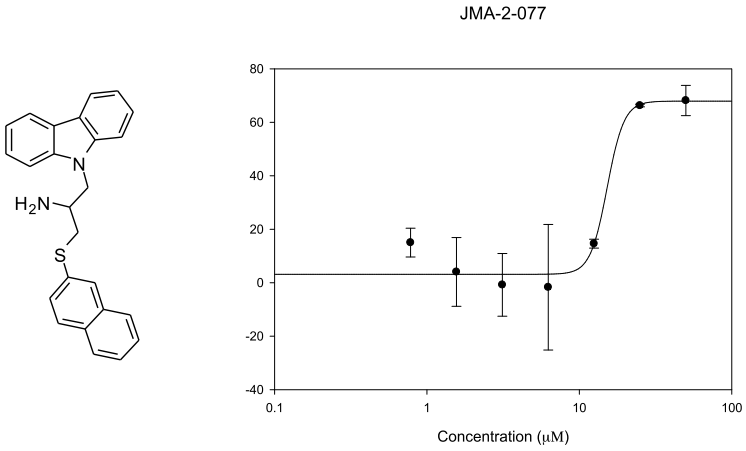

Percent Inhibition at 100 µM

This graph shows the percent inhibition between the coupled product of the epoxides A–R and thiol A"–W".

				50%	60%	70%	80%	90%	Percent Inhibition at 100 µM									
	A	B	C	D	E	F	G	H	I	J	K	L	M	N	O	P	Q	R
A"	79.5	83.1	23.2	84	73.6		74.9	68.6		7.9		23.7	34	74.3	-13.2		66.5	77.1
B"	87.7	95.5	29.7		45.2		85.3	83.2				19.6	10	86.7	-8.8		47.8	69.5
C"	85.7	68.9	1.4				85.3		2.3				-3.6		-18.6			
D"	78.2			82.3	24	88.7		76.8	16.6	30.3		-26.6	65.5		37.8		72.4	81.6
E"																		
F"													21.9				63.3	
G"	64.1	92.9		58.3	70.9		87	86.1	-61.3	18.8		44.9	-26.5		-8		61.9	53.4
H"				53.8				85.6	9.6			15.1	1.5	87.1			62	
I"									-28.9			2.8	24.1		10.4	16.4	63.2	81.8
J"							95.9	-15.8					16					
K"													10.9					
L"		99.7						98.9					44.7	92.2	5.1		81.3	
M"	89.1	55.7				32.1	93.9					23.2	0.9	95.4	8		63.7	
N"								89.7	14.5			14.9	38.4		7		71.3	
O"				71.7				91.9				20.9			-0.9		69.2	78.5
P"												1.1	53.5		-2.9		70.6	79.9
Q"	100	54.7				47.1												73
Y"							51											
S"												15	48.4		13.4			
T"		61.2	17.8	23.9	33.4			32.4		27.2			2		38		83.8	85.5
U"		74.5			17.4					37.5					19		93.5	85.9
V"					26.5		91.2					10.5	6.7		10.5			76.1
W"					74		91.6			1		24.1			5.4			66.8

Percent Inhibition at 50 µM

This graph shows the percent inhibition between the coupled product of the epoxides A–R and thiol A"–W".

				50%	60%	70%	80%	90%	Percent Inhibition at 50 µM									
	A	B	C	D	E	F	G	H	I	J	K	L	M	N	O	P	Q	R
A"	68.7	37.3		75.6														41.7
B"	72.2	70.4					74	54.1						90				
C"	84.8						64											
D"	80.7			94.6		86.3		39										79.5
E"																		
F"																		
G"		64.4					76.2	46.4										
H"								41.2						92				
I"																		69.4
J"							81.3											
K"																		
L"		93.3						87.2						98.5			72.7	
M"	83.7						82							86.2				
N"								70.5										
O"								61.1										78
P"																		72.4
Q"	87.3																	
Y"																		
S"																		
T"																	101	102
U"																	100	77.1
V"							80.9											65.3
W"							88.7											

Percent Inhibition at 25 μM

This graph shows the percent inhibition between the coupled product of the epoxides A–R and thiol A”–W”.

	50%	60%	70%	80%	90%	Percent Inhibition at 25 μM										
	A	B	C	D	E	F	G	H	I	J	K	L	M	N	O	P	Q	R
A”	21.6	-11.4		42.6														20.9
B”	37.5	25.6					27.1	11.29						57.8				
C”	78.8						35.1											
D”	59.6			81.4		39.5		51.8										72.7
E”																		
F”																		
G”		31.4					37.2											
H”								48.2						56.2				
I”																		55.7
J”							52.6											
K”																		
L”		68.2						64.8						67.8			62.3	
M”	67.2						50.7							68				
N”								39.7										
O”								38										42.5
P”																		60.3
Q”	68.5																	
Y”																		
S”																		
T”																	90.1	86.7
U”																	85.1	72.4
V”							54.8											44.9
W”							72.6											